12 mode, WDM, MIMO-free orbital angular momentum transmission

Ingerslev, Kasper; Gregg, Patrick; Galili, Michael; Da Ros, Francesco; Hu, Hao; Bao, Fangdi; Usuga Castaneda, Mario A.; Kristensen, Poul; Rubano, Andrea; Marrucci, Lorenzo; Rottwitt, Karsten; Morioka, Toshio; Ramachandran, Siddharth; Oxenløwe, Leif Katsuo

Published in:
Optics Express

Link to article, DOI:
10.1364/OE.26.020225

Publication date:
2018

Document Version
Publisher's PDF, also known as Version of record

Research Article | Vol. 26, No. 16 | 6 Aug 2018 | OPTICS EXPRESS 20225
Optics EXPRESS

12 mode, WDM, MIMO-free orbital angular momentum transmission

KASPER INGERSLEV,[1,*] PATRICK GREGG,[2] MICHAEL GALILI,[1] FRANCESCO DA ROS,[1] HAO HU,[1] FANGDI BAO,[1] MARIO A. USUGA CASTANEDA,[1] POUL KRISTENSEN,[3] ANDREA RUBANO,[4] LORENZO MARRUCCI,[4] KARSTEN ROTTWITT,[1] TOSHIO MORIOKA,[1] SIDDHARTH RAMACHANDRAN,[2] AND LEIF KATSUO OXENLØWE[1]

[1]*DTU Fotonik, Technical University of Denmark, DK-2800, Lyngby, Denmark*
[2]*Electrical and Computer Engineering Department, Boston University, 8 St Mary's St, Boston, MA, USA*
[3]*OFS-Fitel, Priorparken 680, DK-2605, Broendby, Denmark*
[4]*Dipartimento di Fisica, Università di Napoli Federico II, MSA, via Cintia, 80126 Napoli, Italy*
[*]*kaing@fotonik.dtu.dk*

Abstract: Simultaneous MIMO-free transmission of 12 orbital angular momentum (OAM) modes over a 1.2 km air-core fiber is demonstrated. WDM compatibility of the system is shown by using 60, 25 GHz spaced WDM channels with 10 GBaud QPSK signals. System performance is evaluated by measuring bit error rates, which are found to be below the soft FEC limit, and limited by inter-modal crosstalk. The crosstalk in the system is analyzed, and it is concluded that it can be significantly reduced with an improved multiplexer and de-multiplexer.

OCIS codes: (060.2330) Fiber optics communications; (080.4865) Optical vortices; (060.4230) Multiplexing.

References and links

1. D. J. Richardson, J. M. Fini, and L. E. Nelson, "Space-division multiplexing in optical fibres," Nat. Photonics **7**, 354–362 (2013).
2. N. K. Fontaine, R. Ryf, H. Chen, A. V. Benitez, J. E. A. Lopez, R. A. Correa, B. Guan, B. Ercan, R. P. Scott, S. J. B. Yoo, L. Grüner-Nielsen, Y. Sun, and R. J. Lingle, "30 × 30 mimo transmission over 15 spatial modes," in *Optical Fiber Communication Conference,* (Optical Society of America, 2015), p. Th5C.1.
3. F. Feng, X. Jin, D. O'Brien, F. Payne, Y. Jung, Q. Kang, P. Barua, J. K. Sahu, S. ul Alam, D. J. Richardson, and T. D. Wilkinson, "All-optical mode-group multiplexed transmission over a graded-index ring-core fiber with single radial mode," Opt. Express **25**, 13773–13781 (2017).
4. J. Carpenter, B. C. Thomsen, and T. D. Wilkinson, "Degenerate mode-group division multiplexing," J. Light. Technol. **30**, 3946–3952 (2012).
5. L. Wang, R. M. Nejad, A. Corsi, J. Lin, Y. Messaddeq, L. Rusch, and S. LaRochelle, "Linearly polarized vector modes: enabling mimo-free mode-division multiplexing," Opt. Express **25**, 11736–11749 (2017).
6. S. Ramachandran and P. Kristensen, "Optical vortices in fiber," Nanophotonics **2**, 455–474 (2013).
7. N. Bozinovic, Y. Yue, Y. Ren, M. Tur, P. Kristensen, H. Huang, A. E. Willner, and S. Ramachandran, "Terabit-scale orbital angular momentum mode division multiplexing in fibers," Science **340**, 1545–1548 (2013).
8. R. M. Nejad, K. Allahverdyan, P. Vaity, S. Amiralizadeh, C. Brunet, Y. Massadeq, S. LaRochelle, and L. A. Rusch, "Mode Division Multiplexing using Orbital Angular Momentum Modes over 1.4 km Ring Core Fiber," J. Light. Technol. **34**, 4252–4258 (2016).
9. G. Zhu, Z. Hu, X. Wu, C. Du, W. Luo, Y. Chen, X. Cai, J. Liu, J. Zhu, and S. Yu, "Scalable mode division multiplexed transmission over a 10-km ring-core fiber using high-order orbital angular momentum modes," Opt. Express **26**, 594–604 (2018).
10. P. Gregg, P. Kristensen, and S. Ramachandran, "Conservation of orbital angular momentum in air-core optical fibers," Optica **2**, 267 (2015).
11. C. Brunet, P. Vaity, Y. Messaddeq, S. LaRochelle, and L. A. Rusch, "Design, fabrication and validation of an OAM fiber supporting 36 states," Opt. Express **22**, 26117–26127 (2014).
12. K. Ingerslev, P. Gregg, M. Galili, F. D. Ros, H. Hu, F. Bao, M. A. U. Castaneda, P. Kristensen, A. Rubano, L. Marrucci, S. Ramachandran, K. Rottwitt, T. Morioka, and L. K. Oxenløwe, "12 mode, mimo-free oam transmission," in *Optical Fiber Communication Conference,* (Optical Society of America, 2017), p. M2D.1.
13. L. Marrucci, C. Manzo, and D. Paparo, "Optical spin-to-orbital angular momentum conversion in inhomogeneous anisotropic media," Phys. Rev. Lett. **96**, 163905 (2006).

#332534 https://doi.org/10.1364/OE.26.020225
Journal © 2018 Received 28 May 2018; revised 17 Jul 2018; accepted 17 Jul 2018; published 25 Jul 2018

Optics EXPRESS

14. A. M. Yao and M. J. Padgett, "Orbital angular momentum: origins, behavior and applications," Adv. Opt. Photon. **3**, 161–204 (2011).
15. M. Nakazawa, M. Yoshida, and T. Hirooka, "Nondestructive measurement of mode couplings along a multi-core fiber using a synchronous multi-channel otdr," Opt. Express **20**, 12530–12540 (2012).
16. L. Wang, P. Vaity, S. Chatigny, Y. Messaddeq, L. A. Rusch, and S. LaRochelle, "Orbital-angular-momentum polarization mode dispersion in optical fibers," J. Light. Technol. **34**, 1661–1671 (2016).
17. R. Maruyama, N. Kuwaki, S. Matsuo, and M. Ohashi, "Experimental investigation of relation between mode-coupling and fiber characteristics in few-mode fibers," in *Optical Fiber Communication Conference,* (Optical Society of America, 2015), p. M2C.1.
18. X. Wang, S. Yan, J. Zhu, Y. Ou, Z. Hu, Y. Messaddeq, S. LaRochelle, L. A. Rusch, D. Simeonidou, and S. Yu, "3.36-tbit/s oam and wavelength multiplexed transmission over an inverse-parabolic graded index fiber," in *Conference on Lasers and Electro-Optics,* (Optical Society of America, 2017), p. SW4I.3.
19. G. Labroille, B. Denolle, P. Jian, P. Genevaux, N. Treps, and J.-F. Morizur, "Efficient and mode selective spatial mode multiplexer based on multi-plane light conversion," Opt. Express **22**, 15599–15607 (2014).
20. Z. S. Eznaveh, J. C. A. Zacarias, J. E. A. Lopez, Y. Jung, K. Shi, B. C. Thomsen, D. J. Richardson, S. Leon-Saval, and R. A. Correa, "Annular core photonic lantern oam mode multiplexer," in *Optical Fiber Communication Conference,* (Optical Society of America, 2017), p. Tu3J.3.

1. Introduction

In recent years, mode division multiplexing (MDM) has been explored extensively in order to increase the capacity of optical fiber links [1]. In MDM, several spatial modes propagate simultaneously in the same fiber core. During propagation, these fiber modes can mix in the presence of perturbations such as fabrication imperfections or bending. This mixing can be fully compensated using multiple-input multiple-output (MIMO) digital signal processing (DSP), in the absence of mode dependent loss. However, MIMO processing scales in complexity with N^2, where N is the number of modes, including polarization modes, such that e.g. 30 modes requires 30×30 MIMIO equalization [2].

Alternative schemes have been developed to reduce inter-modal mixing, and thus avoid or reduce the use of cost and power intensive MIMO processing. One proposal is mode-group multiplexing, where several groups of near-degenerate modes are used as data channels. This is achieved either by optically pre-compensating to launch a specific superposition of modes for a given fiber [3], or by reduced-complexity MIMO applied to the groups independently [4]. A second proposal is mode multiplexing where every individual mode is used as a data channel in a fiber in which all degeneracies are broken, e.g. elliptical-core fibers [5]. In these cases, scalability in the number of modes have yet to be demonstrated.

Another option for MIMO free MDM is orbital angular momentum (OAM) modes, which are characterized by a helical phase profile, $\exp(iL\phi)$, where ϕ is the azimuthal coordinate and L is the OAM per photon in units of $\hbar$. In addition to OAM, these modes also carry spin angular momentum (SAM), S, in optics typically known as circular polarization, $\sigma^{\pm} = \frac{1}{\sqrt{2}}(\hat{x} \pm i\hat{y})$, such that the total angular momentum J is given by $J = L + S$. OAM fiber modes come in pairs with OAM and circular polarization of the same sign (spin-orbit aligned) or different sign (spin-orbit anti-aligned), such that four orthogonal modes exist for each $|L| > 1$. With appropriate fiber design, such modes are separated from their nearest neighbors in effective refractive index (n_{eff}), and have been shown to be propagation-stable on the order of kilometers [6].

Previously, MIMO-free data transmission has been demonstrated with four OAM modes over km-lengths of suitably designed optical fibers [7, 8]. Fiber transmission of eight OAM modes has also been demonstrated over longer lengths, though this required the use of MIMO [9]. However, considering that fibers supporting a larger number of OAM states have been designed and tested [10, 11], the number of modes used for OAM MDM can be increased.

This work investigates MIMO-free MDM transmission of 12 OAM modes, and is an extension of our previous report [12]. This is the highest number of modes transmitted MIMO-free over a fiber longer than 1 km. We demonstrate compatibility with wavelength-division multiplexing (WDM), by using a 25 GHz spaced frequency comb with 60 channels modulated with 10 GBaud

Optics EXPRESS

QPSK. We find that all measured data channels achieves bit error rates (BERs) below the soft-decision forward error correction (SD-FEC) limit, and that the system performance is limited by intermodal crosstalk. This crosstalk is analyzed, in terms of in-fiber crosstalk contributions, and mux/demux contributions, in order to identify which parts of the system is limiting the performance.

2. Experimental setup

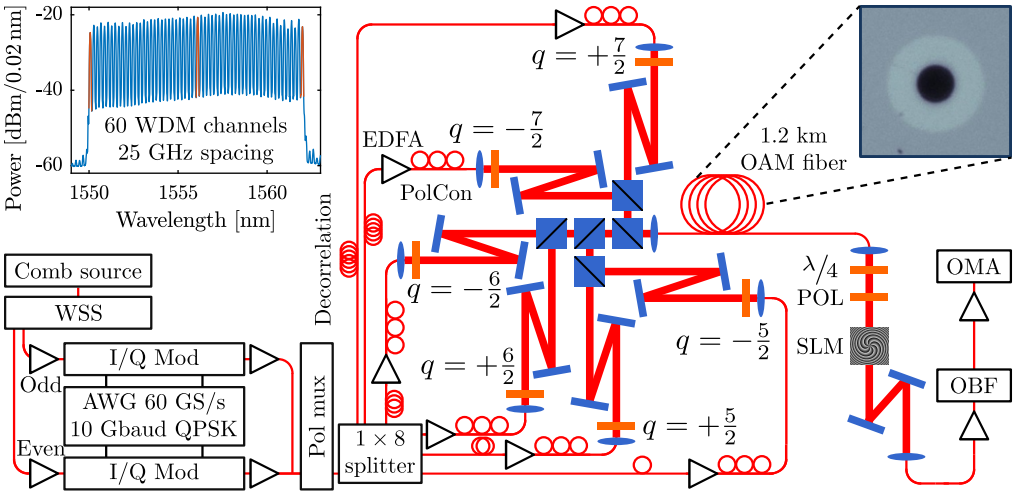

Fig. 1. Schematic of the experimental setup, including the modulated spectrum (top left inset), and a microscope image of the OAM fiber (top right inset). WSS: Wavelength Selective Switch, AWG: Arbitrary Waveform Generator, SLM: Spatial Light Modulator, OBF: Optical Bandpass Filter, OMA: Optical Modulation Analyzer, q: q-plate, PolCon: Polarization Controller, POL: Linear Polarizer, $\lambda/4$: Quarter-wave Plate.

The experimental setup is shown in Fig. 1. A frequency comb of 60 WDM channels with a 25 GHz spacing, spanning from 1550 nm to 1562 nm is generated, by using a 1544 nm continuous wave (CW) laser, which is phase- and then intensity modulated at 25 GHz. This creates initial sidebands, which are amplified and broadened in two stages of highly nonlinear fiber, resulting in a broad comb. The comb is long pass filtered at 1550 nm, since the part of the spectrum near the seed wavelength has low optical signal to noise ratio (OSNR). The amplitude of the 60 WDM channels are equalized, and odd and even channels are split using a wavelength selective switch (WSS). The upper limit of 1562 nm was chosen since it is the maximum wavelength allowed by our erbium doped fiber amplifiers (EDFAs), while the lower limit of 1550 nm is chosen since the fiber does not support all 12 OAM modes at shorter wavelengths. The fiber was designed for enhanced intermodal splitting for OAM modes of $|L| = 5, 6$, and 7, which also determines the launched mode orders in the experimental system. This splitting is enabled via a ring fiber design with large refractive index steps [10].

Odd and even channels are separately amplified and modulated with 10 GBaud QPSK signals, before being amplified again, and recombined in a 3 dB polarization maintaining coupler. This results in 60 single-polarization WDM channels with odd and even decorrelation. Polarization multiplexing is emulated by splitting the signal in two, rotating and delaying one part by ~ 1.5 ns, and then recombining in a polarization beam-splitter. Finally, the signal is split in a 1x8 coupler, 2 outputs are discarded while the remaining 6 polarization multiplexed outputs are amplified separately and temporally decorrelated.

Optics EXPRESS

The 12 OAM modes are generated and multiplexed in free space. Each of the 6 amplified outputs is passed through a polarization controller, collimated into free space, and passed through a q-plate [13], which is a liquid crystal based half-wave plate with a fast axis rotating as a function of the azimuthal angle. The q-plate generates a polarization dependent set of free space OAM modes, by transforming the light such that an input of σ^- is converted to $L = -2q, \sigma^+$ and σ^+ is converted to $L = +2q, \sigma^-$. Thus, the sign of the q-value dictates if the q-plate generates spin-orbit aligned, or spin-orbit anti-aligned modes. In both cases, a superposition of circular polarizations at the input is converted to a superposition of two degenerate OAM modes at the output.

The polarization of the light in each of the six outputs into free space is adjusted, using the polarization controllers, in order to generate a linear combination of the degenerate states, such that the desired OAM modes are detected at the fiber output. This is needed such that the modes can be separated by the mode filter, which is described later. This means that each signal is not mapped onto a pure circular polarization state at the input of the fiber, but rather to a linear combination of the two degenerate modes. During transmission in the fiber, perturbations lead to a unitary transformation, rotating these polarizations, such that pure circular polarization states are detected at the output. This polarization rotation is similar to what happens in a single-mode fiber (SMF), although the perturbation required to achieve a polarization rotation is significantly larger in OAM modes [10]. This means that unlike in SMF, the polarization does not have to be realigned even if the fiber is exposed to small movements.

All of the six beams are individually aligned using silver mirrors, and combined using five 3 dB plate beam-combiners, before being coupled into the OAM fiber using a lens ($f = 8$ mm), with a coupling loss of ~ 2.5 dB. Since the beams pass through a different number of beam combiners, the loss is different for each free-space path, therefore the signal powers are equalized using the six EDFAs. Ultimately this results in a total of 12 multiplexed modes; $L = \pm 5, \sigma^\pm$, $L = \pm 5, \sigma^\mp$, $L = \pm 6, \sigma^\pm$, $L = \pm 6, \sigma^\mp$, $L = \pm 7, \sigma^\pm$, and $L = \pm 7, \sigma^\mp$.

The 12-mode signal is transmitted over a 1.2 km OAM fiber [10] and at the output, the 12 OAM modes are measured one at a time, using a mode filter. This is achieved by passing the light through a circular polarizer comprising a quarter-wave plate with the fast axis oriented at 45° relative to the transmission axis of a linear polarizer. After this step, 6 of the 12 modes remain, each with unique L values. The desired mode is projected onto a mode with $L = 0$ using a spatial light modulator (SLM) with a spiral phase pattern, generated from an azimuthal phase, matching the desired mode, and a parabolic phase, giving a lensing effect. This mode is coupled into a SMF, which acts as a pinhole, filtering the remaining five undesired modes [14].

Finally, the signal is amplified, and a single WDM channel is filtered out with a tunable band-pass filter. The signal, now containing only a single data channel, is amplified again, and sent to an optical modulation analyzer (OMA) that handles demodulation, digital signal processing, and error counting.

The system is aligned using a picosecond pulsed laser source and a 5 GHz free space photodiode, to measure the temporal impulse response of each of the six paths independently [15]. Since the fiber modes have different β_1 values (inverse group speed), this reveals how much power is coupled into each of the 6 non-degenerate modes, with a dynamic range of ~ 20 dB, examples of these measurements can be found in [10]. Afterwards, the polarization of each path is aligned by temporarily removing one output polarization from the polarization multiplexer, and adjusting the polarization controller such that projection into one degenerate state is minimized across the frequency comb, by using a circular polarizer and an optical spectrum analyzer. The polarization was stable, and thus did not need further adjustments during the process of alignment and data transmission. It is observed that while it is easy to get a strong suppression at a single wavelength, it is not always possible to achieve strong suppression of degenerate states across the entire comb. This may be due to either imperfect input coupling, or in-fiber mode coupling [16].

Optics EXPRESS

3. Results and discussion

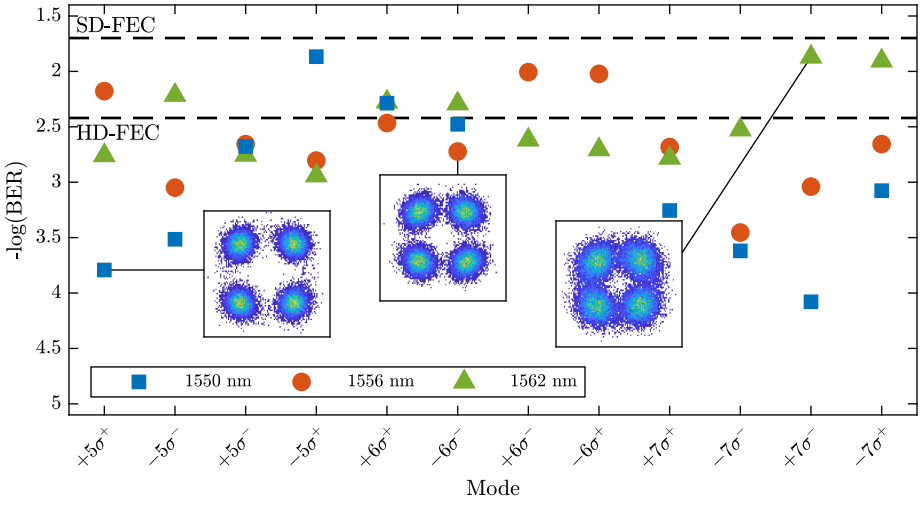

Fig. 2. Measured BERs with example constellation diagrams, from the 3 different wavelengths, 3 different mode groups, and corresponding to low, middle, and high BERs (inset). All 34 measured modes are below the SD-FEC limit, and it is noted that data from the $L = \pm 6, \sigma^{\mp}$ (anti-aligned) modes is missing at 1550 nm, due to accidental degeneracies in the fiber.

System performance was evaluated by measuring BERs at 3 different wavelengths, 1550 nm, 1556 nm, and 1562 nm, corresponding to the comb's shortest, center, and longest wavelength, respectively. All measurements were performed with all 60 wavelengths and 12 modes present in the fiber. The results are shown in Fig. 2, with example constellation diagrams, from the 3 different wavelengths, 3 different mode groups, and corresponding to low, middle, and high BERs. All 34 measured channels are below the soft decision forward error correction threshold (SD-FEC) of 2×10^{-2}, while 24 are below the hard-decision FEC threshold of 3.8×10^{-3}.

It is noted that data from the $L = \pm 6, \sigma^{\mp}$ (anti-aligned) modes is missing at 1550 nm. As seen in Fig. 3(a) this mode (top red line) experiences accidental degeneracies with double ringed, $m = 2$ modes (dashed black lines). This leads to significant multipath interference (MPI), and thus these two modes could not be detected at this wavelength. At the other two measured wavelengths, all 12 modes were detected. By design, this fiber should have experienced no mode crossing for any of the 12 modes. Thus, it is possible that future fabrications of this fiber would yield transmission in all 12 modes across the C-band.

The main limitation to the system performance was intermodal crosstalk. In order to analyze this, the system transmission matrix was measured, and results are shown in Fig. 3(b). Each column corresponds to an output projection setting, while each row indicates which modes are launched and thus contribute to crosstalk at the receiver. It is seen that total crosstalk (top row in Fig. 3(b)) into each of the modes was measured to be between -10.3 dB and -11.8 dB. This crosstalk has two main contributions, namely in fiber mode coupling, and crosstalk at the mux/demux. By comparing the middle and bottom rows in 3(b), it was found that the strongest parasitic contribution for the $|L| = 5$ modes is in-fiber crosstalk between the $|L| = 5$ spin-orbit aligned and anti-aligned modes (-12.8 dB), because this mode group has the smallest n_{eff} splitting of 6×10^{-5}. This analysis also reveals that the $|L| = 6$ and $|L| = 7$ modes are mainly limited by crosstalk from modes of different $|L|$. As seen in Fig. 3(a), the n_{eff} splitting between L and $L \pm 1$ is an order of magnitude larger than between modes with the same $|L|$, therefore in-fiber mode coupling between adjacent OAM mode orders is unlikely to be significant at ~ 1 km [17], and

Optics EXPRESS

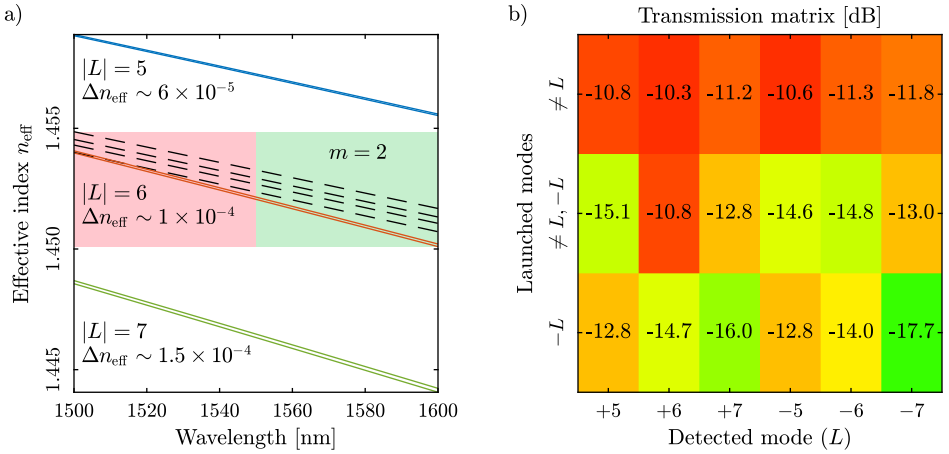

Fig. 3. a) Simulated n_{eff} as a function of wavelength, the red shaded area denotes the bandwidth where the $|L| = 6$ anti-aligned modes have strong MPI. b) System transmission matrix where each column corresponds to an output projection setting, while the rows correspond to modes launched. Each column is normalized to 0 dB in the desired mode with entries denoting crosstalk in dB. $-L$ indicates crosstalk from in-fiber nearest neighbors, $\neq L, -L$ indicates contributions from other mode orders, and $\neq L$ indicates total crosstalk. Crosstalk is measured using the frequency comb, yielding an average for the used optical spectrum.

thus it is concluded that this MPI is primarily due to imperfections in the free-space mux/demux. Furthermore, significant temporal drifting of the mux/demux was observed, leading to cross-talk increasing with time, thus limiting the number of measurements that could be performed before re-alignment is needed.

Assuming that all 30 WDM channels between 1550 nm and 1556 nm fail to carry the $|L| = 6$ spin-orbit anti-aligned modes, and thus only support 10 modes, while the 30 longer wavelength channels support 12 modes, the demonstrated system may potentially have a total aggregate capacity of 10.56 Tbit/s after 20% FEC overhead has been deducted for all channels. Compared to previous fiber-based OAM transmission systems, this corresponds to a 6-fold improvement in capacity compared to [7], or a 3-fold improvement in capacity, and a 12-fold improvement in distance compared to [18].

4. Crosstalk analysis

To improve the understanding of the crosstalk contributions, namely in-fiber crosstalk, and mux/demux crosstalk, they are further analyzed. In the mux, crosstalk comes mainly from misalignments, where the input beam is shifted compared to the fiber end facet. In order to compute how much power is coupled into each fiber mode, the normalized overlap integral between the free space field and each fiber mode is computed for different spatial offsets. At perfect alignment, the input field is matched with a single fiber mode, and is orthogonal to the remaining modes. However, a misalignment (shift in spatial position) results in parasitic mode excitation.

To do this, the fiber modes were solved using a finite difference frequency domain mode solver. A total of 52 guided modes were found at 1555 nm (26 in each polarization), where 12 are the desired OAM modes, and the remaining 40 are lower order modes that do not propagate stably in the fiber, but must be included in these calculations. The overlap of each desired mode (simulating the input beam) with all of the 52 modes (simulating the fiber) is computed, then the input field

Optics EXPRESS

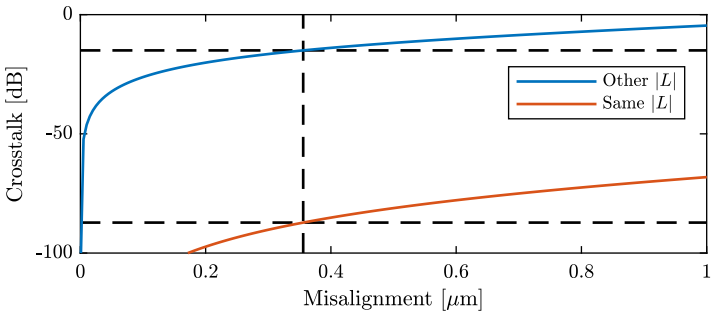

Fig. 4. Simulated maximum crosstalk to modes with different $|L|$ and modes with the same $|L|$ as a function of input misalignment. Crosstalk is defined as the amount of power coupled to an undesired mode, divided by the power coupled to the desired mode.

is shifted along the x-axis, and the computations are repeated. Because of circular symmetry, shifting the input along a single axis is sufficient.

The results are shown in Fig. 4, where the maximum crosstalk contributions for the 12 desired modes are plotted. The crosstalk is split into contributions to modes with other $|L|$, and the same $|L|$ i.e. inter-group crosstalk and intra-group crosstalk, respectively. The maximum crosstalk is chosen as a figure of merit since it ensures that all spatial channels perform within a given threshold. The individual modes behave similarly to the maximum, and are within 1 dB of the maximum for the case of other $|L|$, and within 4 dB in the case of same $|L|$. It is seen that in order to have a maximum crosstalk of -15 dB (corresponding to the measured values in Fig. 3(b)) the maximum allowed alignment error is 350 nm. At this tolerance, the crosstalk contribution to modes with the same $|L|$ is -87 dB, thus concluding that misalignments in the mux/demux only affects crosstalk to modes with other $|L|$. This crosstalk mainly goes to neighboring modes with same polarization and same handedness, i.e. when trying to excite $L = +7\sigma^+$ the main undesired mode will be $L = +6\sigma^+$. This, along with the fact that the $|L| = 6$ modes has two neighbors, explains why they perform worse than the $|L| = 5$, modes, even though they have a larger n_{eff} splitting.

In addition to crosstalk from misalignments, crosstalk from polarization mixing in the free space optics should also be considered. Since the fields are circularly polarized, it is impossible to align them to either the s- or p-axis of the optical components, as would be done with linear polarization. Therefore, any difference in the complex reflection (or transmission) coefficients of the mirrors and beam combiners transforms the polarization from circular to elliptical. This corresponds to a coupling between the two orthogonal polarization states σ^+ and σ^-, without affecting the OAM, thus resulting in crosstalk from spin-orbit aligned modes to spin-orbit anti-aligned modes. This crosstalk contribution is estimated to ~ -25 dB based on time of flight measurements and specifications of the optical components. Compared to the measured spin-orbit aligned to spin-orbit anti-aligned crosstalk for the full system (shown in Fig. 3(b)), this is an order of magnitude lower. Thus, it is concluded that the majority of the crosstalk to modes with the same $|L|$ does not come from the mux/demux, and therefore must originate in the fiber.

To examine in-fiber crosstalk, further measurements were performed, by transmitting a set of four modes with the same $|L|$, and thereby only looking at crosstalk within this group. As concluded above, this should reduce the effects of mux/demux crosstalk by an order of magnitude. Since in-fiber crosstalk depends on the difference in effective refractive index, Δn_{eff}, the impact can be predicted by studying Fig. 3(a). It is seen that modes with different $|L|$ have $\Delta n_{\text{eff}} \sim 5 \times 10^{-3}$, while the aligned and anti-aligned pairs have $\Delta n_{\text{eff}} \sim 6 \times 10^{-5}$, $\Delta n_{\text{eff}} \sim 1 \times 10^{-4}$, and $\Delta n_{\text{eff}} \sim 1.5 \times 10^{-4}$ for $|L| = 5$, $|L| = 6$, and $|L| = 7$, respectively. Thus it is expected

Optics EXPRESS

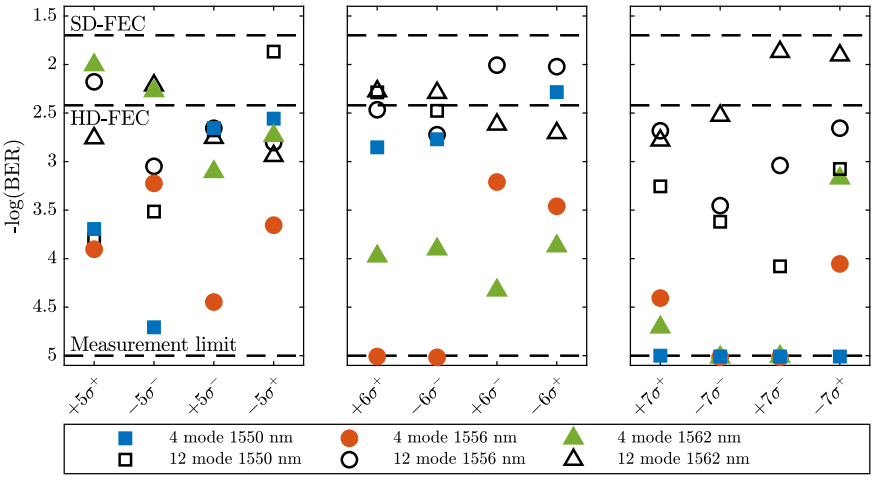

Fig. 5. Measured BERs for sets of four modes with same $|L|$ (colored markers) and the 12-mode measurements from Fig. 2 for reference (black hollow markers).

that in-fiber crosstalk should be most significant for the $|L| = 5$ modes, and least significant for the $|L| = 7$ modes, while in-fiber crosstalk to modes with different $|L|$ should be virtually nonexistent.

These results are shown in Fig. 5 using colored points, while the 12-mode results, from Fig. 2 are shown in black for comparison. It is seen that the BERs in the 4-mode case are better than in the 12-mode case. In the case of $|L| = 6$, and $|L| = 7$ all of measured 4-mode BERs are better than the corresponding 12-mode measurements, while in the case of the $|L| = 5$ modes, 8 of the 12 modes has lower BERs than the corresponding 12-mode measurements. Additionally, it is seen that the BERs match the predictions based the simulated Δn_{eff}, thus confirming that in-fiber crosstalk is the limiting factor in the 4-mode measurements. This also means that mux/demux crosstalk was a main limiting factor in the 12-mode transmission, and thus if an ideal mux/demux was used, the 12-mode BERs could be expected to be as low as the 4-mode BERs. In the future, new multiplexers based on multi-plane light conversion [19], or photonic lanterns [20] could solve this problem.

5. Summary and conclusions

12 OAM modes, each carrying a 10 GBaud QPSK signal have been transmitted over a 1.2 km air-core fiber. WDM compatibility was demonstrated by using a comb source with 60 WDM channels with 25 GHz spacing. This is the largest number of modes over which MIMO-free data has been transmitted over a fiber longer than 1 km. The most significant limitations encountered in this demonstration were the difficulties and drifts associated with aligning 6 free-space optical arms with high accuracy. Crosstalk was analyzed in terms of in-fiber contributions and contribution from the mux/demux, and it was concluded that the mux/demux was the main limiting factor. Thus it is expected that developments in mux/demux technologies would significantly enhance the system performances and capacity of MIMO-free data transmission using OAM fiber modes.

Funding

Danish National Research Foundation Centre of Excellence SPOC (DNRF213); Innovations Fonden e-space (0603-00514B); Office of Naval Research (ONR) MURI (N0014-13-1-0672); National Science Foundation (NSF) (DGE-1247312, ECCS-1610190).